

Synthesis of ZnS whiskers and their photoluminescence properties*

Du Yuanyuan(杜园园)[†], Jie Wanqi(介万奇), and Li Huanyong(李焕勇)

(School of Materials Science and Engineering, Northwestern Polytechnical University, Xi'an 710072, China)

Abstract: ZnS whiskers were successfully synthesized by the chemical vapor deposition method with the assistance of CuS micro-spheres. The composition, morphology and structure of the samples were characterized by X-ray diffraction, X-ray energy dispersive spectroscopy, scanning electron microscopy, and the temperature-dependent photoluminescence (PL) spectrum over a temperature range from 10 to 250 K was studied. The results show that the as-synthesized ZnS whiskers have an average length of 0.3 mm and diameter of 2.5 μm with a cubic zinc-blende structure. There exist three emission bands in the blue, green and yellow regions, and the emission mechanism is discussed. As the temperature increases, the temperature-dependent PL spectrum shows anomalous behavior, where distinct inverted V-shaped characters of blue and green emission integrated intensity and an inconspicuous S-shape of blue emission peak energy are observed. The transition mechanism is discussed.

Key words: chemical vapor deposition; ZnS whiskers; anomalous; luminescence

DOI: 10.1088/1674-4926/30/8/083005

PACC: 7280E; 8115H

1. Introduction

One-dimensional (1D) semiconductor nanomaterials have attracted much attention due to their special physical properties and potential applications in opto-electronic nanodevices and functional materials. As a well-known direct wide-band-gap semiconductor compound, ZnS is one of the most promising materials for fabricating optoelectronic devices, such as electroluminescent devices, optical inter-band transition devices, flat-panel displays, infrared windows, alpha-particle monitoring devices, sensors and lasers^[1-4]. Recently, extensive studies have been carried out on the synthesis and physical properties of low-dimensional structures, such as nanowires, nanorods, nanobelts, nanotubes and nanowhiskers. As ZnS whiskers have better optical properties without unfavorable effects on optical transmission, several methods have been developed to prepare them, such as the low-temperature organometallic route, the metallic zinc sulfidation route^[5,6], and calcination of zinc sulfate, KCl and active carbon at high temperatures^[7]. However, as a simple and inexpensive method for industrial production, chemical vapor deposition (CVD) has seldom been reported. So it is urgent for scientists to explore economical and simple methods to synthesize fine ZnS whiskers.

In this paper, we report a simple CVD method to synthesize fine ZnS whiskers for the first time. The morphology, structure and photoluminescence (PL) properties of the as-synthesized samples are studied.

2. Experiment

ZnS whiskers were massively synthesized in a simple horizontal CVD system. Zinc powder (A.R.) and CuS micro-

spheres served as the starting materials. All the reagents were of analytic purity and used without any further purification. The CuS micro-spheres were prepared according to Ref. [8] and the obtained CuS precipitate was evenly distributed on a clean silicon wafer and dried in a vacuum box at 50 °C for several hours. Subsequently, the CuS-coated Si substrate and a quartz crucible filled with Zn powder were placed in a clean quartz tube, and the whole quartz tube was inserted into a horizontal furnace. With the introduction of 50–200 sccm of high purity Ar gas, the furnace was heated and maintained at about 550 °C for 60 min. After the furnace was cooled to room temperature, white powder was found covering the whole silicon wafer.

The synthesized sample was characterized by X-ray diffraction (XRD, Panalytical X'pert PRO), scanning electron microscopy (SEM, Hitachi S-570) and X-ray energy dispersive spectroscopy (EDS, INCA) to determine its morphologies and crystal structures. For the PL spectrum, a continuous wave He–Cd laser with a wavelength of 325 nm and a power of 50 mW was used as the excitation source, and the luminescence signals were detected with a TRIAX 550 spectrometer from Jobin Yvon.

3. Results and discussion

Figure 1 shows the XRD spectrum of as-synthesized ZnS whiskers grown on Si (100). All the diffraction peaks are in good agreement with cubic zinc-blende ZnS with a crystal constant of $a = 0.5411$ nm, which matches well with the standard value of bulk ZnS crystal within experimental errors (JCPDS Card No. 5-5066). The sharp diffraction peaks indicate that the as-synthesized product has good crystal quality.

* Project supported by the National Natural Science Foundation of China (Nos. 50502028, 50336040).

[†] Corresponding author. Email: duyuy1983@163.com, duyuyuan@mail.nwpu.edu.cn

Received 18 December 2008, revised manuscript received 18 March 2009

© 2009 Chinese Institute of Electronics

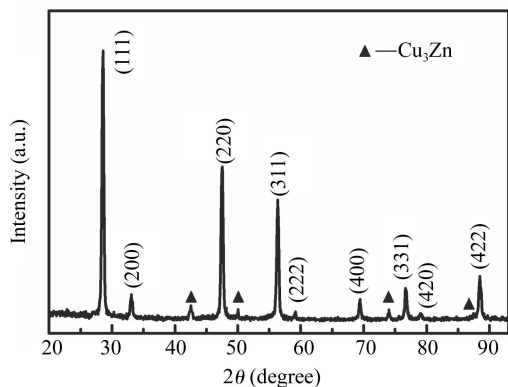


Fig. 1. XRD pattern of as-synthesized ZnS whiskers.

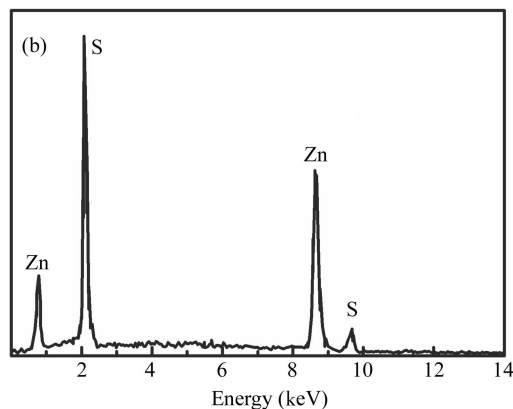
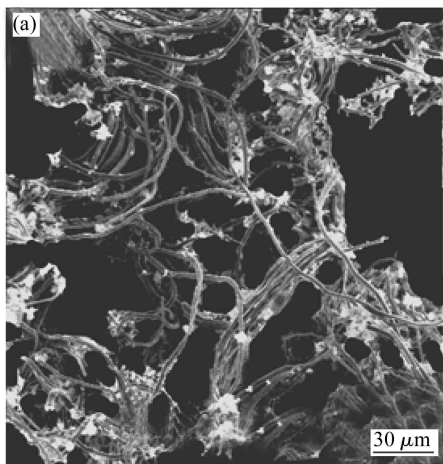


Fig. 2. (a) SEM image and (b) EDS spectrum of the body of ZnS whiskers.

In addition, no diffraction peaks of other crystalline impurities are detected in the sample, except those peaks of Cu_3Zn alloy from resource reagents, which are situated at 43.50°C , 50.37°C , 74.04°C , and 89.78°C , corresponding to its (111), (200), (220) and (311) faces, respectively.

Figure 2(a) shows an SEM photo of the ZnS whiskers. It can be seen that the whiskers are uniformly distributed on Si substrate with random orientation, and are crooked and entwined with each other. In addition, a small amount of ZnS particles attached to the whiskers is observed. The length of the whiskers is between 0.3 and 0.5 mm with an average diameter of $0.25\ \mu\text{m}$, indicating that it is possible to obtain super-long ZnS whiskers with the assistance of CuS micro-spheres. The composition of the ZnS whiskers measured by the EDS

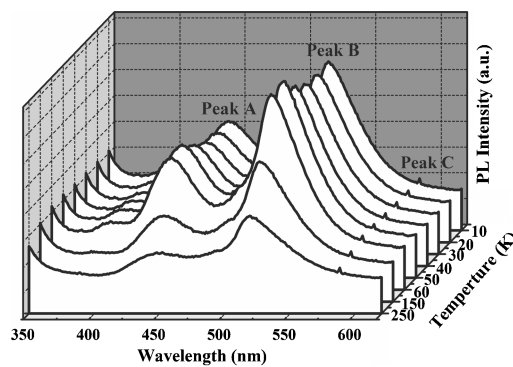


Fig. 3. PL spectra of ZnS whiskers with excitation wavelength at 325 nm in the temperature region 10–250 K.

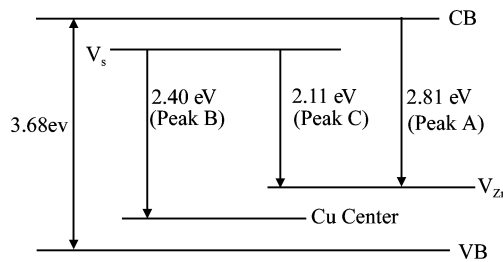


Fig. 4. Schematic energy level diagram of the emission mechanism in ZnS whiskers.

spectrum is shown in Fig. 2(b); the atomic ratio of Zn to S is about 1.09 : 1, which reveals that the obtained ZnS whisker is close to an ideal stoichiometric composition. It can be predicted that the growth mechanism of ZnS whiskers could be explained by the vapor-liquid-solidification (VLS) mechanism referred to in the research of Li *et al.*^[9] and the alloy particle at the tip of the ZnS whiskers is Cu_3Zn alloy.

Figure 3 shows the photoluminescence spectrum of ZnS whiskers in the region from 350 to 600 nm measured at different temperatures from 10 to 250 K. It shows that there are two distinct peaks situated in the blue region about 442.5 nm (peak A) and the green region about 518 nm (peak B), respectively, and one inconspicuous peak (peak C, about 588 nm) located in the yellow region, which has seldom been reported in the literature. The 442.5 nm blue emission is due to recombination between the conduction band and zinc vacancy-related acceptor^[10], while the 518 nm green peak is attributed to recombination between the sulfur vacancy (V_S) related donor and Cu related acceptor center^[11]. According to the results of XRD and the EDS spectrum shown in Fig. 2, sulfur vacancies and Cu_3Zn in the samples are identified. Considering that Cu atoms can substitute Zn in the Zn sites and act as acceptors in the form of Cu_3Zn , we can certainly attribute the 588 nm yellow emission to recombination between V_S and the zinc vacancy-related acceptor. In the ZnS whiskers, the number of sulfur vacancies is more than that of zinc vacancies and Cu related acceptor centers can act as nonradiative recombination centers; thus, green emission is dominant in the PL spectrum. Based on the above results, a schematic energy level diagram of the emission mechanism in ZnS whiskers is depicted, as shown in Fig. 4, to explain the emission mechanism of ZnS whiskers and illustrate the aforementioned arguments.

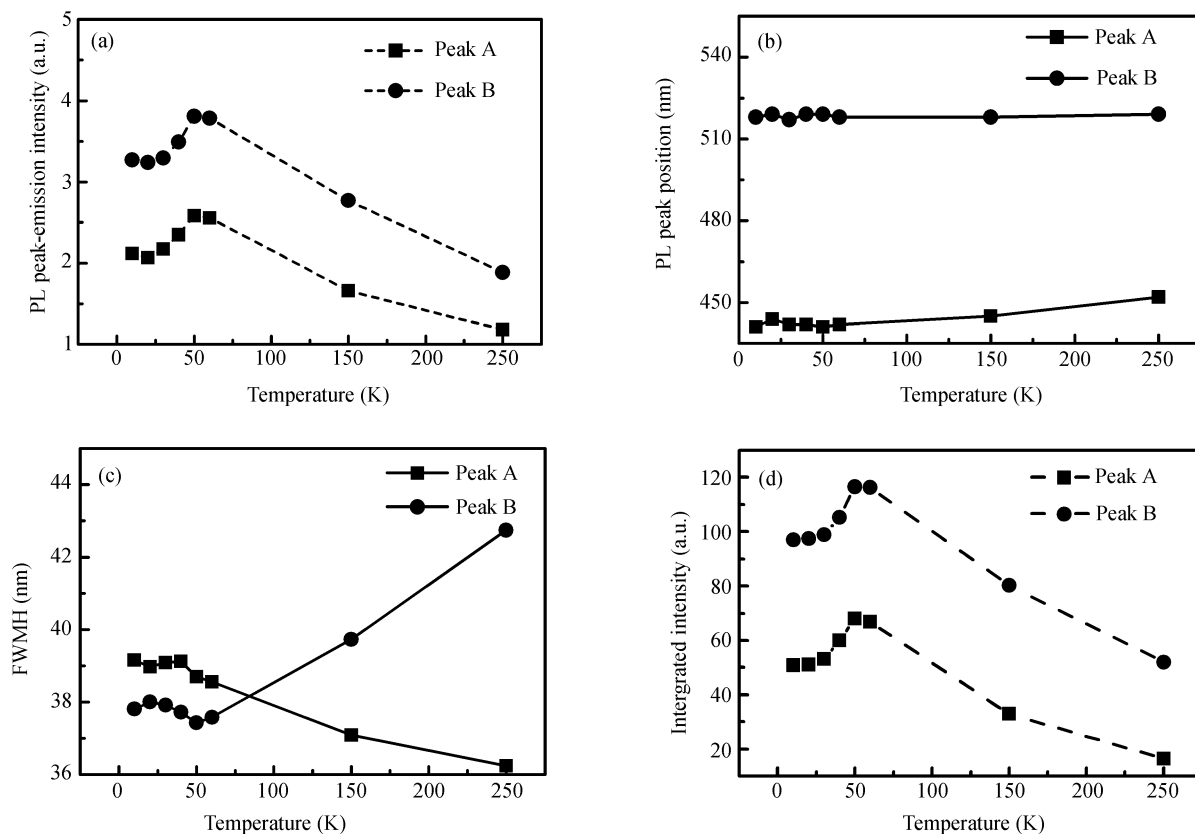


Fig. 5. Temperature-dependent PL spectra of ZnS whiskers: (a) PL peak-emission intensity; (b) PL peak-emission position; (c) FWHM; (d) Integrated intensity. Peak A is the blue peak, and Peak B is the green peak.

From Fig. 3, it can be seen that the PL spectrum shape of the ZnS whiskers is almost independent of the temperature change, but the intensity of peaks A and B increases as temperature increases to 50 K, and then starts to decrease gradually, as shown in Fig. 5(a). This is anomalous because in a general PL spectrum, the peak-emission intensity diminishes gradually as temperature increases; the reason for this will be analyzed later in detail.

In order to study the effect of temperature for the PL emission peak of ZnS whiskers concretely, the spectrum is well fitted by two Gaussian peaks and the correlation coefficients are larger than 0.96. A plot of the peak position against temperature is shown in Fig. 5(b). The peaks A and B undergo a small redshift as the temperature increases to 20 K. Peak A shifts from 441 to 444 nm, while peak B shifts from 518 to 519 nm. Beyond 20 K, both of the two peaks undergo a small blueshift and then a redshift again. Peak A shows no monotonic and an inconspicuous S-shape for temperature-dependence of the PL emission peak position, while peak B is kept almost stable as temperature increases. Similar temperature-induced S-shape shift behavior was also observed in lots of materials, such as AlGaIn^[12], GaInNAs^[13] and ZnO nanoneedle arrays^[14], which are reported to be attributed to the effect of carrier localization in the materials. The S-shaped shift of peak A in this article is the process of “redshift–blueshift–redshift”. From 10 to 20 K, a redshift appears, because the holes in the zinc vacancy-related acceptor gain thermal energy, overcome energy barriers and recombine

with the electrons in the conduction band; meanwhile, this redshift is also influenced by temperature-induced band-gap shrinkage. The blueshift from 20 to 50 K is caused by the thermal population effect of holes localized at the zinc vacancy-related acceptor, while the influence of band-gap shrinkage is totally counteracted by the localization effect. At temperatures beyond 50 K, the redshift is mainly determined by band-gap shrinkage. Therefore, the S-shaped shift of the blue emission could be based on the competition results between the hole localization effect of temperature induced at the zinc vacancy and band-gap shrinkage.

The full-width at half-maximum (FWHM) variations with temperature were calculated and plotted in Fig. 5(c). Unlike most of the measurements for semiconductors, the result does not exhibit a monotonous increase with increasing temperature: the FWHM of peak A shows an increasing broadening in the 10 to 40 K temperature interval, reaching a maximum at 40 K, and a decrease at higher temperatures, which is similar to the PL FWHM on temperature of CdTe/CdSe core-shell type-II quantum dots^[15]. We consider that the increase of FWHM at low temperatures is a result of thermal broadening, while the decrease at high temperatures is due to the fact that most of the holes of zinc vacancies are accumulated in the ground states and emit photons; thus the emission is dominated by the recombination of delocalized states of the excitons and the linewidth narrows. The FWHM of peak B decreases and then increases upon varying the temperature from 10 to 250 K: the turning point is at around 50 K, and we think

that the initial decrease in FWHM may be due to the gradual ionization of Cu impurities and that the subsequent increase is due to thermal broadening with increasing temperature.

The integrated intensity of the photoluminescence versus temperature for peaks A and B is plotted in Fig. 5(d). We can see that the integrated intensity of the two peaks shows anomalous inverted V-shaped characters with increasing temperature. In general, the PL intensity decreases with increasing temperature due to a reduction of excitonic transitions with temperature. The characteristic exhibited by the integrated intensity of the PL peak—a maximum at some measurement temperatures—has also appeared in other materials, such as porous silicon^[16], a-C:H film^[17], silicon nanocrystals in SiO₂^[18] and stoichiometric Gd₂O_{3-x} film^[19]. In this article, the integrated intensity of the peaks increases at first, reaches its maximum at about 50 K, and finally starts to diminish gradually. An enhancement of phonon-assisted indirect radiative recombination in this indirect-band-gap material is proposed to explain the former anomalous temperature dependence of optical emission^[20], while the latter can be ascribed to a reduction of excitonic transitions with increasing temperature.

4. Conclusions

We have successfully synthesized ZnS whiskers using a simple CVD method, and CuS micro-spheres have served as the catalyst for the first time. The as-synthesized ZnS whiskers are 2.5 μm in average diameter and 300 μm in length, with zinc-blende structure. Anomalous photoluminescence properties of the ZnS whiskers, depending on temperature have been observed, and detailed observations on PL emission mechanism, peak intensity, peak position, FWHM and PL integrated intensity are reported. There exist three emission bands in the blue, green and yellow regions. With increasing temperature, both the PL peak intensity and integrated intensity of the blue and green emission show a distinct inverted V-shaped character, which can be ascribed to the enhancement of phonon-assisted indirect radiative recombination. The temperature-dependence of the blue emission peak energy showing an inconspicuous S-shape is the result of the competition between the hole localization effect of temperature induced at the zinc vacancy and band-gap shrinkage. The anomalous behaviors of the blue and green emission FWHM are due to the carrier redistribution and the gradual ionization of impurities, respectively.

References

- [1] Shen G Z, Bando Y, Golberg D. Self-assembled three-dimensional structures of single-crystalline ZnS submicrotubes formed by coalescence of ZnS nanowires. *Appl Phys Lett*, 2006, 88(12): 123107
- [2] Denzler D, Olschewski M, Sattler K. Luminescence studies of localized gap states in colloidal ZnS nanocrystals. *J Appl Phys*, 1998, 84(5): 2841
- [3] Ding Y, Wang X D, Wang Z L. Phase controlled synthesis of ZnS nanobelts: zinc blende vs wurtzite. *Chem Phys Lett*, 2004, 398: 32
- [4] Geng B Y, Liu X W, Du Q B, et al. Structure and optical properties of periodically twinned ZnS nanowires. *Appl Phys Lett*, 2006, 88(16): 163104
- [5] Guiton T A, Pantano C G. Synthesis of ZnS whiskers. *Solid State Ionics*, 1989, 32/33: 506
- [6] Czekaj C L, Rau M S, Geoffroy G L, et al. An organometallic route to micron-sized whiskers of zinc sulfide. *Inorg Chem*, 1988, 27(19): 3267
- [7] He Y L, Wang J K. A novel simple method to prepare ZnS whiskers. *Mater Lett*, 2008, 62: 1379
- [8] Deng H, Chen C, Peng Q, et al. Formation of transition-metal sulfide microspheres or microtubes. *Mater Chem Phys*, 2006, 100: 224
- [9] Li Huanyong, Jie Wanqi, Xiong Peng, et al. Vapor growth of one-dimensional ZnE (E = S, Se) nanowires. *Rare Metal Materials and Engineering*, 2007, 36(Suppl. 2): 279 (in Chinese)
- [10] Jayanthi K, Chawla S, Chander H, et al. Structural, optical and photoluminescence properties of ZnS: Cu nanoparticle thin films as a function of dopant concentration and quantum confinement effect. *Cryst Res Technol*, 2007, 42(10): 9760
- [11] Lee S, Song D, Kim D J, et al. Effects of synthesis temperature on particle size/shape and photoluminescence characteristics of ZnS : Cu nanocrystals. *Mater Lett*, 2004, 58: 342
- [12] Bell A, Srinivasan S, Plumlee C, et al. Exciton freeze-out and thermally activated relaxation at local potential fluctuations in thick Al_xGa_{1-x}N layers. *J Appl Phys*, 2004, 95: 467
- [13] Grenouillet L, Bru-Chevallier C, Guillot G. Evidence of strong carrier localization below 100 K in a GaInNAs/GaAs single quantum well. *Appl Phys Lett*, 2000, 76: 2241
- [14] Cao B Q, Cai W P, Zeng H B. Temperature-dependent shifts of three emission bands for ZnO nanoneedle arrays. *Appl Phys Lett*, 2006, 88: 161101
- [15] Wang C H, Chen T T, Tan K W, et al. Photoluminescence properties of CdTe/CdSe core-shell type-II quantum dots. *J Appl Phys*, 2006, 99(12): 123521
- [16] Perry C H, Lu F. Photoluminescence spectra from porous silicon (111) microstructures: temperature and magnetic-field effects. *Appl Phys Lett*, 1990, 60(25): 3117
- [17] Liao M Y, Feng Z H, Yang S Y, et al. Anomalous temperature dependence of photoluminescence from a-C:H film deposited by energetic hydrocarbon ion beam. *Solid State Commun*, 2002, 121: 287
- [18] Brongersma M L, Kik P G, Polman A, et al. Size-dependent electron-hole exchange interaction in Si nanocrystals. *Appl Phys Lett*, 2000, 76(3): 351
- [19] Zhou J P, Chai C L, Yang S Y, et al. Anomalous temperature dependence of photoluminescence from stoichiometric Gd₂O_{3-x} film. *J Cryst Growth*, 2004, 260: 136
- [20] Kwack H S, Sun Y P, Choa Y H. Anomalous temperature dependence of optical emission in visible-light-emitting amorphous silicon quantum dots. *Appl Phys Lett*, 2003, 83(14): 2901